Editors' Suggestion | Featured in Physics

Giant Photocaloric Effects across a Vast Temperature Range in Ferroelectric Perovskites

Riccardo Rurali,[1] Carlos Escorihuela-Sayalero,[2,3] Josep Lluís Tamarit,[2,3] Jorge Íñiguez-González,[4,5] and Claudio Cazorla[2,3]

[1]Institut de Ciència de Materials de Barcelona, ICMAB–CSIC, Campus UAB, 08193 Bellaterra, Spain
[2]Departament de Física, Group of Characterization of Materials, Universitat Politècnica de Catalunya, Campus Diagonal-Besòs, Avenida Eduard Maristany 10–14, 08019 Barcelona, Spain
[3]Research Center in Multiscale Science and Engineering, Universitat Politècnica de Catalunya, Campus Diagonal-Besòs, Avenida Eduard Maristany 10–14, 08019 Barcelona, Spain
[4]Luxembourg Institute of Science and Technology (LIST), Avenue des Hauts-Fourneaux 5, L-4362 Esch/Alzette, Luxembourg
[5]Department of Physics and Materials Science, University of Luxembourg, 41 Rue du Brill, L-4422 Belvaux, Luxembourg

(Received 8 April 2024; accepted 18 July 2024; published 10 September 2024)

Solid-state cooling presents an energy-efficient and environmentally friendly alternative to traditional refrigeration technologies that rely on thermodynamic cycles involving greenhouse gases. However, conventional caloric effects face several challenges that impede their practical application in refrigeration devices. First, operational temperature conditions must align closely with zero-field phase-transition points; otherwise, the required driving fields become excessively large. However, phase transitions occur infrequently near room temperature. Additionally, caloric effects typically exhibit strong temperature dependence and are sizable only within relatively narrow temperature ranges. In this Letter, we employ first-principles simulation methods to demonstrate that light-driven phase transitions in polar oxide perovskites have the potential to overcome such limitations. Specifically, for the prototypical ferroelectric $KNbO_3$ we illustrate the existence of giant "photocaloric" effects induced by light absorption ($\Delta S_{PC} \sim 100\ J\,K^{-1}\,kg^{-1}$ and $\Delta T_{PC} \sim 10$ K) across a vast temperature range of several hundred Kelvin, encompassing room temperature. These findings are expected to be generalizable to other materials exhibiting similar polar behavior.

DOI: 10.1103/PhysRevLett.133.116401

Solid-state cooling is an environmentally friendly and highly energy-efficient technology that harnesses caloric effects in materials for refrigeration purposes [1]. Through the application of external fields to caloric materials, large reversible entropy and temperature changes ($\Delta S \sim 10$–$100\ J\,K^{-1}\,kg^{-1}$ and $\Delta T \sim 1$–10 K) can be achieved, seamlessly integrated into cooling cycles without reliance on greenhouse gases. Particularly, polar materials undergoing paraelectric to ferroelectric phase transitions under small electric fields are well suited for solid-state cooling applications based on the electrocaloric (EC) effect [2–4], which can be miniaturized and coherently integrated into electronic circuits.

For caloric phenomena to be integrated in practical applications, the underlying zero-field phase transitions must occur close to room temperature. Otherwise, the necessary driving fields may reach impractically high levels, creating an energetically unfavorable scenario and worsening the materials performance due to the appearance of leakage and/or eddy currents, dielectric-magnetic losses, and mechanical fatigue. Unfortunately, only few compounds exhibit phase transitions near room temperature, which limits the range of solid-state refrigeration applications. Additionally, caloric effects normally exhibit a strong dependence on temperature, being substantial only within relatively narrow temperature intervals.

In this Letter, we propose a solution to the described caloric material challenges by focusing on polar to nonpolar phase transitions triggered by light absorption [5]. In addition to the promising photoferroelectric phenomena recently reported, such as optically induced reversal of the polarization [6–8] and optically induced triggering of polar order [9], several light-induced polar to nonpolar phase transitions have been experimentally measured. This is the case for polyvinylidene fluoride-multiwalled carbon nanotube nanocomposites, where optical switching between a polar and nonpolar phase has been demonstrated [10], isotope exchanged $SrTi(^{16}O_{1-x}{}^{18}O_x)_3$, where photoinduced suppression of its ferroelectric transition has been claimed [11], $Ba_{0.875}(Bi_{0.5}Li_{0.5})_{0.125}TiO_3$, where a significant photoinduced change in the dielectric permittivity and decrease in the Curie temperature have been reported [12], and very recently freestanding $BaTiO_3$ membranes, where photostriction has been linked to the suppression of the ferroelectric polarization by photoexcited carriers [13].

Here, we theoretically demonstrate the existence of giant photocaloric (PC) effects ($\Delta S_{PC} \sim 100\ J\,K^{-1}\,kg^{-1}$ and $\Delta T_{PC} \sim 10$ K) in the archetypal ferroelectric $KNbO_3$

(KNO). These PC effects persist across a vast temperature range spanning several hundred Kelvin, including room temperature, and are comparable to state-of-the-art EC effects [2–4]. The substantial anharmonicity of the paraelectric phase, naturally occurring at high temperatures ($\gtrsim$700 K [14,15]), coupled with its stabilization through light irradiation, are the primary factors responsible for the unravelled giant PC effects.

Density functional theory (DFT) calculations [16,17] were performed using the semilocal Perdew-Burke-Ernzerhof approximation for solids (PBEsol) [18]. Electric polarizations were estimated with the Born effective charges method [19]. Photoexcitation was mimicked by constraining the partial occupancies of the electronic orbitals via adjustment of the Fermi distribution smearing [5,20,21]. Thermal expansion effects were accounted for with the quasiharmonic approximation (QHA) [22,23]. DFT Gibbs free energies were computed with the QHA method considering T-renormalized phonons [24] for the dynamically unstable phases at zero temperature ("DFT-rQHA"). Additional details of our calculations are in Supplemental Material [25].

The ground state of KNO is a polar rhombohedral phase ($R3m$, R). At temperatures of $220 \leq T \leq 470$ K, KNO stabilizes in a polar orthorhombic phase ($Amm2$, O) [14,15]. Upon absorption of above-band-gap light, some valence electrons in KNO are photoexcited and promoted to the conduction band, where they gain increased mobility and become delocalized throughout the crystal. These carriers effectively screen the long-range dipole-dipole interactions that are key to the existence of polar order in the ferroelectric phase. Consequently, the nonpolar cubic phase ($Pm\bar{3}m$, C), which is stable at temperatures $T \gtrsim 700$ K under dark conditions [14,15], becomes the ground state under "light" conditions [Fig. 1(a)].

Our zero-temperature DFT calculations reveal that the nonpolar C phase becomes vibrationally stable at photoexcited electronic densities exceeding $\bar{n} = 2.69 \times 10^{21}$ cm^{-3} [Fig. 1(b)], which mainly are accommodated in oxygen $2p$ orbitals (Supplemental Material Fig. 1 [25]). Importantly, our DFT simulations demonstrate that both the polar R and O phases spontaneously relax into the nonpolar C phase under sufficiently high light irradiation (or, equivalently, density of photoexcited electron-hole pairs). Consequently, under such photoexciting conditions, the polar phases R and O are unstable rather than metastable, thus suggesting ultrafast dynamics for the proposed light-induced polar to nonpolar phase transition [21].

In this Letter, above-band-gap light absorption is crucial since it drives the photoexcitation of charge carriers. Hence, in practice, the light frequency range should be ultraviolet ($h\nu \geq E_g^{\mathrm{KNO}} \approx 3$ eV [31]). An essential parameter for the practical feasibility of the described photoinduced phase-transition mechanism is the light penetration length, Δz. If Δz is too small, the light-induced phase transition may not occur homogeneously unless $\Delta z \sim L$, where L represents a

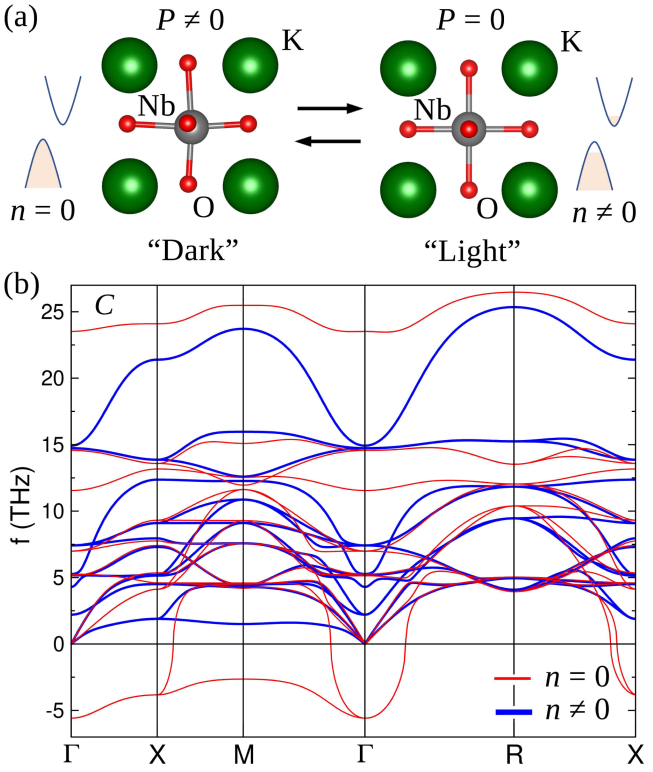

FIG. 1. Light-driven phase-transition mechanism in ferroelectric $KNbO_3$. (a) Upon photoexcitation, electrons are promoted to the conduction band and ferroelectric KNO transforms into a nonpolar cubic phase C. (b) Vibrational phonon spectrum of $KNbO_3$ in the nonpolar C phase at $T = 0$ K conditions in the absence (red lines) and presence (blue lines) of photoexcited electrons ($\bar{n} = 2.69 \times 10^{21}$ cm^{-3}).

characteristic size of the sample. Based on experimental optical absorption data for KNO [31], we estimate $\Delta z \approx 30$ μm, which significantly exceeds the usual thickness of oxide perovskite thin films (~0.1–1.0 μm). Therefore, for practical implementations of the photocaloric phenomena unveiled in this Letter, films are the most advisable systems. Additional factors possibly affecting the homogeneity of the light-induced phase transition in KNO are commented on in the Supplemental Material discussion [25].

According to our first-principles DFT calculations, the polar R phase is characterized by a lattice parameter of 4.034 Å, rhombohedral angle of 89.89°, and ferroelectric polarization of $P = 35.05$ μC cm^{-2}. These results compare remarkably well with the corresponding experimental values ($T = 230$ K) of 4.016 Å, 89.83°, and 30–40 μC cm^{-2}, respectively [14,32,33]. For the polar O phase, we estimated the unit cell parameters $a = 3.996$ Å, $b = c = 4.053$ Å, $\alpha = 90.18°$, and $\beta = \gamma = 90°$, and a ferroelectric polarization of $P = 38.53$ μC cm^{-2} along the pseudocubic direction [011]. These calculated values are also in very good agreement with the corresponding

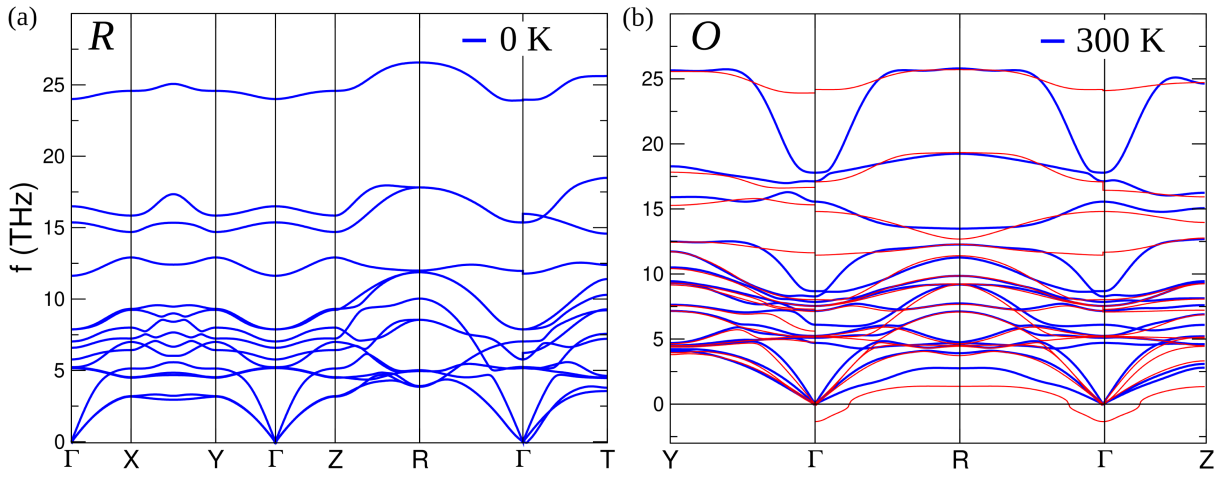

FIG. 2. Phonon spectrum of $KNbO_3$ in the polar R and O phases ("dark" conditions). The R phase is dynamically stable at zero temperature (a), whereas the O phase is not, thin red lines in (b). The T-renormalized phonon spectrum of the O phase renders dynamical stability at room temperature (blue lines) in agreement with the experiments [14,15].

experimental results ($T = 295$ K) 3.973 Å, 4.035 Å, 90.27°, and $\approx 40\ \mu C\,cm^{-2}$ [14,32,33]. Therefore, the employed DFT approach offers a robust description of KNO.

Figure 2 displays the phonon spectrum of the polar R and O phases at dark conditions. In the case of the O phase, the phonon frequencies were renormalized to account for thermal effects at room temperature using a normal-mode decomposition method [24]. Our computational results accurately replicate the dynamical stability observed in experiments for the polar R and O phases at low and room temperature, respectively [14,15].

The Gibbs free energy (G) of the polar R and O phases was estimated with a numerical uncertainty of approximately 1 meV per formula unit (f.u.), based on the size of the supercells and technical parameters of the employed DFT-rQHA approach. The $R \rightarrow O$ phase-transition temperature T_t is determined from the condition $G_O(T_t) = G_R(T_t)$. We found that, considering the numerical uncertainties of 1 meV/f.u., and given the proximity in energy (near degeneracy) of the two polymorphs, the G of the R and O phases could not be distinguished in the temperature range $0 \leq T \lesssim 200$ K (Fig. 3). However, at higher temperatures, it is clearly appreciated that $G_O < G_R$. Consequently, from our calculations it can be assuredly concluded that the polar O phase becomes stable at temperatures above ≈ 200 K (Fig. 3), which is in reasonable agreement with the experimental transition temperature of 220 K [14,15].

Subsequently, the entropy $S = -\partial G/\partial T$ of the R, O, and C phases was computed as a function of temperature and light irradiation conditions, denoted as $S(T, x)$ (where $x = d$, l stand for dark and light conditions, respectively). The resulting $S(T, x)$ curves exhibit smooth behavior, as explicitly shown in Figs. 4(a) and 4(b). Analogous to quasidirect calorimetry experiments [34,35], the photocaloric isothermal entropy ΔS_{PC} and adiabatic temperature changes ΔT_{PC} can be readily inferred from these entropy curves [36]. In particular, $\Delta S_{PC} = S(T, l) - S(T, d)$ and $\Delta T_{PC} = T_0(S, l) - T(S, d)$, where T_0 fulfills the condition $S(T_0, l) = S(T, d)$ [black solid lines in Figs. 4(a) and 4(b)].

Figure 4 shows examples of ΔS_{PC} and ΔT_{PC} evaluations, considering the temperature intervals in which the polar R and O phases are observed to be thermodynamically stable. For instance, at $T \approx 220$ K and considering the R phase under dark conditions [Fig. 4(a)], we estimated a giant isothermal entropy change of $89.5\ J\,K^{-1}\,kg^{-1}$ and an adiabatic temperature change of -8.0 K ($\Delta T_{PC} < 0$ since the phase stabilized with light has higher entropy). Similarly, at room temperature and considering the O phase under dark conditions [Fig. 4(b)], we computed a

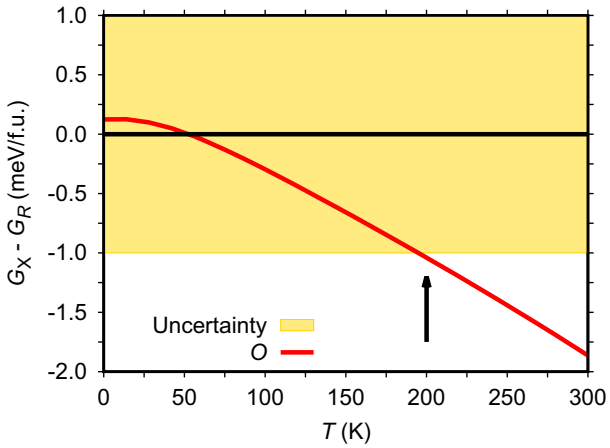

FIG. 3. DFT-rQHA prediction of the T-induced $R \rightarrow O$ phase transition in $KNbO_3$. The Gibbs free energy of the R and O phases cannot be distinguished in the temperature range $0 \leq T \lesssim 200$ K, taking into account the numerical uncertainties of 1 meV per formula unit. The polar O phase is predicted to become stable at temperatures $\gtrsim 200$ K (arrow) in fair agreement with the experiments [14,15].

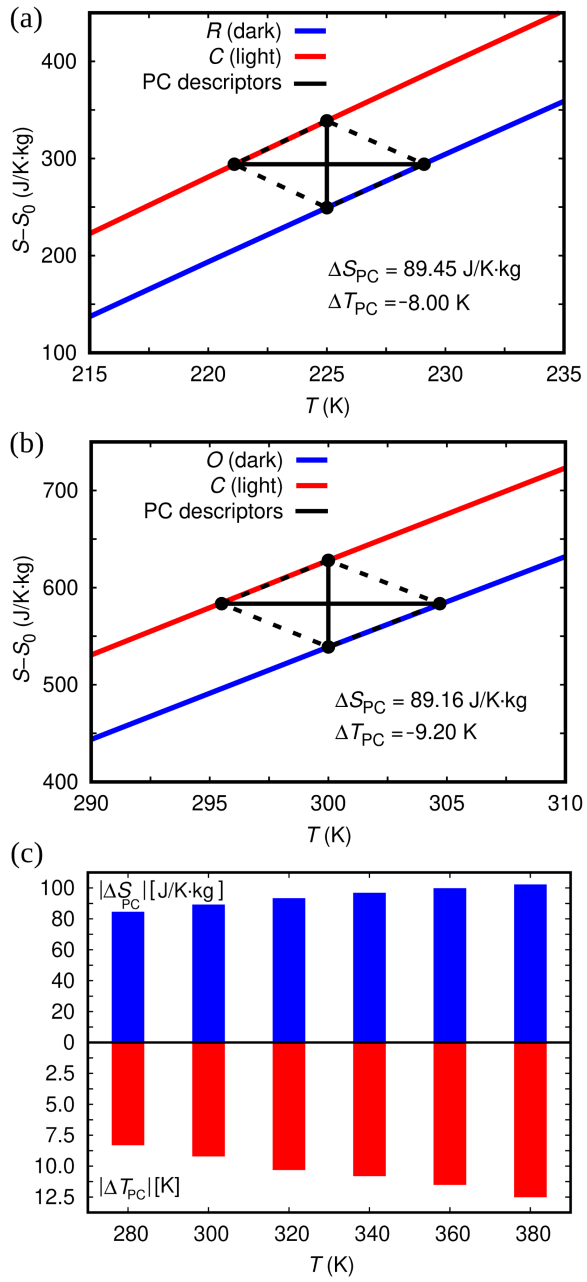

FIG. 4. Evaluation of photocaloric effects in $KNbO_3$. (a) For the polar R (dark) and nonpolar C (light) phases. (b) For the polar O (dark) and nonpolar C (light) phases. ΔS_{PC} and ΔT_{PC} are straightforwardly determined from the entropy curves (black solid lines). (c) Summary of the photocaloric results obtained over a vast temperature interval.

substantial isothermal entropy change of 89.2 $J\,K^{-1}\,kg^{-1}$ and an adiabatic temperature change of −9.2 K.

These photocaloric results are highly promising for technological applications as they are comparable in size to state-of-the-art EC effects [2–4]. Specifically, the magnitude of the $|\Delta T_{PC}|$ predicted for KNO is approximately one order of magnitude larger than the $|\Delta T_{EC}|$ measured for similar polar materials such as $BaTiO_3$ [37]. The relatively large $|\Delta T_{PC}|$ as compared to $|\Delta T_{EC}|$ (or, equivalently, $|\Delta S_{PC}| > |\Delta S_{EC}|$) can be attributed to the unique nature of the proposed light-induced phase transition: the nonpolar C phase is directly stabilized, bypassing the intermediate polar states that are typically encountered during conventional T-induced transformations [14,15]. Consequently, polar materials similar to KNO, that is, presenting high Curie temperatures, are probably most suitable for achieving substantial photocaloric responses.

A highly promising aspect of the photocaloric effect theoretically unveiled in this Letter, which sets it apart from other known caloric effects, is its operability over vast temperature intervals defined by the ranges of thermodynamic stability of the material polar phases. This exceptional characteristic is explicitly demonstrated in Fig. 4(c), where we represent the $|\Delta S_{PC}|$ and $|\Delta T_{PC}|$ estimated for KNO over an unprecedented wide temperature range spanning more than 100 K and encompassing room temperature. Interestingly, both the isothermal entropy and adiabatic temperature changes slightly, but steadily increase with increasing temperature. For example, at $T = 380$ K, these quantities amount to 102.2 $J\,K^{-1}\,kg^{-1}$ and 12.50 K, respectively. This behavior is due to the fact that the variation of entropy upon increasing temperature, or equivalently, the heat capacity $C_p = T(\partial S/\partial T)_p$, is larger for the nonpolar C phase (Supplemental Material Fig. 2 [25]).

The likely persistence of PC effects down to very low temperatures makes the proposed scheme an appealing alternative for achieving cryogenic temperatures, as one can envision sequential cooling cycles working at increasingly lower temperatures. This type of cryogenic cooling could be particularly useful in applications such as quantum computing. However, this possibility deserves further theoretical exploration, due to the inevitable consideration of quantum nuclear effects [23].

A possible four-step refrigeration cycle based on the photocaloric effect predicted here for KNO is envisioned, as shown in Figs. 5(a) and 5(b).

(0) → (1) adiabatic light exposure: Initially, starting from the polar low-entropy O phase at room temperature T_0, the KNO system is adiabatically irradiated until stabilizing the nonpolar high-entropy C phase. As a result, the temperature of the KNO sample decreases, $T_1 < T_0$ ($\Delta T_{PC} < 0$).

(1) → (2) heat transfer: With the light conditions maintained, the KNO sample is placed in contact with the targeted body to be refrigerated, facilitating the transfer of heat toward KNO, $|Q| = T \cdot |\Delta S_{PC}|$, until restoring its initial temperature conditions, $T_2 = T_0$.

(2) → (3) adiabatic light removal: The light is adiabatically switched off, stabilizing the polar low-entropy O phase again. Consequently, the temperature of the KNO sample increases, $T_3 > T_0$.

(3) → (0) heat removal: Finally, the KNO sample is placed in contact with a heat sink, allowing heat to flow

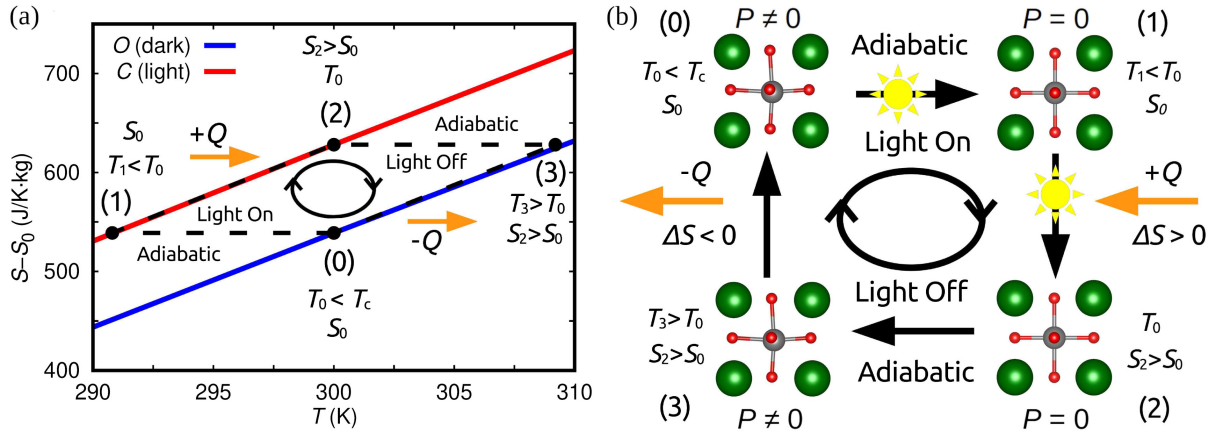

FIG. 5. Envisaged solid-state refrigeration cycle. A possible four-step solid-state refrigeration cycle based on the photocaloric effect unveiled in this Letter is illustrated (a) quantitatively with entropy curves and (b) qualitatively with a diagram.

from KNO until restoring the initial temperature conditions, thereby completing a cooling cycle.

A rough estimation of the coefficient of performance (COP) associated with this refrigeration cycle amounts to 1, which despite being promising still is not competitive with respect to commercial refrigeration devices, typically exhibiting COPs of 10 (Supplemental Material discussion [25]). Additional practical aspects of the proposed PC cooling cycle are commented on in the Supplemental Material discussion [25].

In conclusion, we have presented compelling theoretical evidence for the existence of giant photocaloric effects driven by light absorption in the archetypal ferroelectric perovskite $KNbO_3$. The magnitude of the unveiled photocaloric effects is remarkably large, that is, comparable to the most promising electrocaloric effects measured in ferroelectrics. An unparalleled and distinctive feature of these photocaloric effects is that they remain very large over vast temperature intervals spanning several hundred Kelvin, only limited by the ranges of thermodynamic stability of the polar phases of the material. Therefore, this Letter provides motivation for exploring new concepts and strategies to develop environmentally friendly and highly miniaturizable solid-state cooling technologies.

Acknowledgments—We acknowledge financial support by the Spanish Ministry of Science under the Grants No. PID2020–119777 GB-I00, No. TED2021-130265B-C22, No. PID2020–112975 GB-I00, No. RYC2018-024947-I and by the Generalitat de Catalunya under the Grants No. 2021SGR-00343 and No. 2021SGR-01519. This work is part of the Severo Ochoa Excellence Programme (CEX2023-001263-S). Computational support was provided by the Red Española de Supercomputación under the Grants No. FI-2023-2-0004, No. FI-2023-3-0043, and No. FI-2024-1-0005. This work is part of Maria de Maeztu Units of Excellence Programme CEX2023-001300-M funded by MCIN/AEI/10.13039/501100011033. Work at LIST was supported by the Luxembourg National Research Fund through Grant No. C21/MS/15799044/FERRODYNAMICS.

[1] X. Moya and N. D. Mathur, Science **370**, 797 (2020).
[2] Y. Nouchokgwe, P. Lheritier, Ch. Hong *et al.*, Nat. Commun. **12**, 3298 (2021).
[3] S. E. Shirsath, C. Cazorla, T. Lu *et al.*, Nano Lett. **20**, 1262 (2020).
[4] J. Li, A. Torelló, V. Kovakova *et al.*, Science **382**, 801 (2023).
[5] C. Paillard, E. Torun, L. Wirtz, J. Íñiguez, and L. Bellaiche, Phys. Rev. Lett. **123**, 087601 (2019).
[6] R. Mankowsky, A. von Hoegen, M. Först, and A. Cavalleri, Phys. Rev. Lett. **118**, 197601 (2017).
[7] V. A. Abalmasov, Phys. Rev. B **101**, 014102 (2020).
[8] V. A. Abalmasov, Phys. Rev. B **104**, L140102 (2021).
[9] X. Li, T. Qiu, J. Zhang *et al.*, Science **364**, 1079 (2019).
[10] P. Viswanath and M. Yoshimura, SN Appl. Sci. **1**, 1519 (2019).
[11] Y. Yamada and K. Tanaka, J. Lumin. **112**, 259 (2005).
[12] S. Pal, A. B. Swain, P. P. Biswas, and P. Murugavel, Phys. Rev. Mater. **4**, 064415 (2020).
[13] S. Ganguly, D. Pesquera, D. Moreno-García *et al.*, Adv. Mater. **36**, 2310198 (2024).
[14] D. Wang, G. Wang, Z. Lu *et al.*, Front. Mater. **7**, 91 (2020).
[15] G. Shirane, R. Newnham, and R. Pepinsky, Phys. Rev. **96**, 581 (1954).
[16] G. Kresse and J. Furthmüller, Phys. Rev. B **54**, 11169 (1996).
[17] P. E. Blöchl, Phys. Rev. B **50**, 17953 (1994).
[18] J. P. Perdew, A. Ruzsinszky, G. I. Csonka, O. A. Vydrov, G. E. Scuseria, L. A. Constantin, X. Zhou, and K. Burke, Phys. Rev. Lett. **100**, 136406 (2008).
[19] César Menéndez and Claudio Cazorla, Phys. Rev. Lett. **125**, 117601 (2020).
[20] B. Peng, Y. Hu, S. Murakami *et al.*, Sci. Adv. **6**, eabd1618 (2020).
[21] C. Cazorla, S. Bichelmaier, C. Escorihuela-Sayalero *et al.*, Nanoscale **16**, 8335 (2024).

[22] A. Togo and I. Tanaka, Scr. Mater. **108**, 1 (2015).
[23] C. Cazorla and J. Boronat, Rev. Mod. Phys. **89**, 035003 (2017).
[24] A. Carreras, A. Togo, and I. Tanaka, Comput. Phys. Commun. **221**, 221 (2017).
[25] See Supplemental Material at http://link.aps.org/supplemental/10.1103/PhysRevLett.133.116401 for a detailed description of the employed computational methods, the electronic density of states and heat capacity of $KNbO_3$, along with a supplemental discussion on possible practical aspects affecting the implementation of the photocaloric effect unveiled in this Letter for solid-state cooling purposes, which includes Refs. [26–30].
[26] G. Ross, G. Montemezzani, P. Bernasconi, M. Zgonik, and P. Günter, J. Appl. Phys. **79**, 3665 (1996).
[27] G. S. García-Quirino, J. J. Sanchez-Mondragon, and S. Stepanov, Phys. Rev. A **51**, 1571 (1995).
[28] A. S. Johnson, D. Perez-Salinas, K. M. Siddiqui *et al.*, Nat. Phys. **19**, 215 (2023).
[29] T. F. Nova, A. S. Disa, M. Fechner *et al.*, Science **364**, 1075 (2019).
[30] P. M. Resende, F. Le Goupil, G. Fleury, and G. Hadziioannou, Phys. Rev. Appl. **21**, 054021 (2024).
[31] Y. Kaifu, T. Komatsu, T. Hirano *et al.*, J. Phys. Soc. Jpn. **23**, 903 (1967).
[32] A. I. Frenkel, F. M. Wang, S. Kelly, R. Ingalls, D. Haskel, E. A. Stern, and Y. Yacoby, Phys. Rev. B **56**, 10869 (1997).
[33] M. D. Fontana, G. Metrat, J. L. Servoin *et al.*, J. Phys. C **17**, 483 (1984).
[34] P. Lloveras, A. Aznar, M. Barrio *et al.*, Nat. Commun. **10**, 1803 (2019).
[35] A. Aznar, P. Negrier, A. Planes *et al.*, Appl. Mater. Today **23**, 101023 (2021).
[36] C. Escorihuela-Sayalero, L. C. Pardo, M. Romanini *et al.*, npj Comput. Mater. **10**, 13 (2024).
[37] F. Han, Y. Bai, L.-J, Qiao *et al.*, J. Mater. Chem. C **4**, 1842 (2016).